METHODOLOGY TO PREDICT STRAIN OF BRIDGING VEIN DUE TO ROTATION OF HEAD

Yukou Takahashi
Toshiyuki Yanaoka
Honda R&D Co., Ltd.
Japan

Paper Number 23-0261

ABSTRACT

The brain stem can be damaged by the herniation of the brain tissue, potentially leading to fatality. Mass lesion could lead to fatality due to brain stem herniation, necessitating the prediction of the strain of the bridging veins (BVs). A number of trabecula forming a web-like structure of the sub-arachnoid space (SAS) may allow the assumption that the strain of the BVs correlates with that of the SAS. The objective of this study is to investigate the predictive capability of the strain in both the brain parenchyma (BP) and the SAS using a simplified physical model based on the CIBIC (Convolution of Impulse Response for Brain Injury Criterion) criterion proposed by the authors.

A viscoelastic model consisting of a series of two sets of standard linear solids (SLSs) used in the CIBIC criterion (extended version of CIBIC; e:CIBIC) was developed to represent both the BP and the SAS. The Global Human Body Models Consortium (GHBMC) head/brain model was used to obtain the target response of the maximum principal strain (MPS) in the BP and the SAS. Three angular acceleration time histories to be used to optimize model parameters were determined by combining twenty sine waves with the frequency ranging 10-200 Hz. The optimization of the spring and damping coefficients was performed by maximizing the CORA (CORrelation and Analysis) score for the time histories of the MPS in the BP and the SAS obtained from the GHBMC model. The optimized e:CIBIC was further assessed against a total of 256 sets of head rotational acceleration time histories obtained from frontal and side impacts and pedestrian impacts. The assessment was performed for the coefficient of determination of the correlation of the peak MPS with the GHBMC model along with the average value of the CORA score with the strain in both the BP and the SAS. The two assessment metrics were also compared against the original CIBIC criterion for the brain strain to clarify improved prediction.

The results of the performance assessment using the two metrics showed that e:CIBIC is capable of simulating the MPS in the BP with an accuracy similar to the original CIBIC. It was also found that the predictive capability of e:CIBIC for the MPS in the SAS is higher than that of the original CIBIC for the MPS in the BP.

This study revealed that e:CIBIC with the two sets of the SLS in series is capable of predicting the strain in both the SAS and the BP simultaneously. The results obtained in this study is dependent upon the validity of the head/brain FE model used. The relationship between the strain of the SAS and the probability of BV failure needs to be further investigated.

INTRODUCTION

Over the last couple of years, the number of traffic fatalities has decreased worldwide, largely due to the traffic volume drop coming from Covid-19 pandemic. According to the OECD report [1], the traffic volume dropped by 12.2% in 2020 compared to the average of 2017-2019 in 11 countries that collect data on travel volume. Consequently, the number of road death decreased by 8.6% across 34 member countries, with the majority of them seeing drop as much as 20%. Similar trend also applies specifically to Japan, with the reduction of the number of traffic fatalities of 18.4% among the same period [2]. Despite this significant decreasing trend in traffic fatalities, head injury is still responsible for the largest proportion in traffic fatality. Japanese accident statistics in 2021 [3] shows that the head accounts for 41.5% in the distribution of the major body part of the physical damage of all fatal accidents. It accounts for even more than half specifically in pedal cyclists (58.2%) and pedestrians (53.3%). Of those head injuries, traumatic brain injury (TBI) plays a significant role. Li et al. [4] reviewed 60 reports from 29 countries with data on TBI epidemiology and found that death was the most common outcome in patients with moderate and severe TBI. Motor vehicle collision (MVC) was the leading cause of TBI in 14 countries, including China, Japan, Australia, France, Spain, Austria,

Netherland and Italy. Such epidemiological findings have facilitated research aiming to establish a methodology to assess TBI in MVC.

In an effort to establish a methodology to assess TBI in MVC, Takahashi et al. [5] investigated the accident data from the National Automotive Sampling System (NASS) Crashworthiness Data System (CDS) from 2010 to 2014 and Pedestrian Crash Data Study (PCDS) from 1994 to 1998, with the head respectively comprising 33% and 46% of all body regions sustaining Maximum Abbreviated Injury Scale (MAIS) in fatal accidents. Of those head injuries, brain injury accounts for 78% and 81% of the head injuries responsible for the death for the data from NASS CDS and PCDS, respectively. Based on the tissue failure and anticipated injury mechanisms, types of TBI were classified into three major categories; pressure and/or skull fracture (brain contusion, epidural hematoma), brain strain (subarachnoid hemorrhage, intracranial hemorrhage and diffuse axonal injury) and displacement relative to the skull (subdural hematoma). The classification showed that TBIs primarily due to strain in the brain are by far most frequent, accounting for 81% and 73% of all TBIs for NASS CDS and PCDS database, respectively. Along with the early study by Holbourn et al. [6] that hypothesized that the shear strain in the brain primarily due to the rotational acceleration of the head is a predominant cause of brain damage due to large bulk modulus of the brain substance compared with its modulus of rigidity, many of recent studies have focused on the prediction of the strain in the brain primarily induced by head rotation in MVC.

In addition to the damage to the brain parenchyma (BP) due to the strain caused by the rotation of the head, the other important mechanism to consider is the rupture of the bridging vein (BV) that leads to acute subdural hematoma (ASDH). The rupture of the BV accumulates the blood between the dura mater and the cortex and generate hematoma that compresses the brain, which would lead very often to long term incapacity and high mortality rates [7]. Some of the studies have focused on detailed FE modeling of BVs to predict rupture of the BV [7][8] to enhance prediction capability of BV rupture. As currently available head/brain FE models generally use a set of simplified one-dimensional bar elements to represent the BVs [9], such detailed FE representation of the BVs would provide a valuable insight in the estimation of potential mechanism of BV rupture and subsequent ASDH. The other way to approach the issue, however, is to model the essential part of the physical phenomena involved in the mechanism of injury by means of a more simplified representation to provide a more practical means of injury assessment. The authors have applied this concept in the prediction of the strain in the BP to develop the CIBIC criterion [5]. It is based on the analytical solution of the response of the standard linear solid (SLS) model with a mass to acceleration time histories in three directions. The assumption was that the simplified viscoelastic model is capable of analogously representing the maximum principal strain (MPS) in the brain of the full-FE head/brain model with the brain tissue modeled using a linear viscoelastic material model. Surprisingly enough, good correlation was seen between the peak MPS predicted by the FE head/brain model and the CIBIC criterion. Subsequently, the same concept was also used by Gabler et al. [10], endorsing a good performance of such kinematics-based simple representation of the peak value of the MPS in the brain tissue. Although the validity of such simplified kinematics-based prediction models depend largely on the validity of the full-FE head/brain model against which model parameters are optimized, they still provide practical means of predicting brain response to impact based on the state-of-the-art prediction of brain injury mechanisms using full-FE simulations. However, to the best of the authors' knowledge, there has been no study that focuses on the prediction of BV rupture using a kinematics-based criterion.

The sub-arachnoid space (SAS) forms one of the three layers called the meninges that encase the brain and spinal cord. Anatomically, the SAS consists of a network of fine delicate connective tissue called sub-arachnoid trabeculae (SAT) that gives this space its characteristic spider web appearance. The SAT act as supportive pillars, allowing the flow of CSF [11]. SAT enclose the small blood vessels and adhere to the surface of larger blood vessels in the SAS and cisterns, providing mechanical support to neurovascular structures through cell-to-cell interconnections and specific junctions between the pia and arachnoid matters [12]. Such anatomical and clinical findings would lead to the assumption that the failure of the BV that goes though the SAS is related to the strain of the SAS in consideration of a simplified and kinematics-based prediction methodology of ASDH.

The goal of this study was to develop a methodology to predict rupture of the BV using a kinematics-based criterion. As the first step toward this ultimate goal, the current study focused on predicting the strain in the SAS along with the

prediction of the strain in the BP by means of extending the function of the CIBIC criterion to develop an extended version of the CIBIC criterion (e:CIBIC).

METHODS

e:CIBIC was developed by adding another set of the SLS in series to the single SLS used for the CIBIC criterion [5] to predict MPS in both the BP and the SAS simultaneously. The model parameters were determined using simplified rotational acceleration time histories to match the MPS in the BP and the SAS predicted by a full-FE 3D head/brain model. Similar to the CIBIC criterion, the numerical computation of e:CIBIC was replaced by the convolution integral to make sure that it yields the same results with a more simple calculation suitable for practical use. Finally, e:CIBIC expressed by the convolution integral procedure was validated against the same FE head/brain model in a number of crash test and simulation results.

Determination of model parameters

Figure 1 shows the comparison of the SLS model used for the CIBIC and e:CIBIC criterion for one particular direction of motion. e:CIBIC incorporates two sets of the SLS model each representing the BP and the SAS. As the lumped mass primarily represents the mass of the brain, and the rotational motion of the skull and the mandible is supposed to be given to the bottom of the lower SLS, displacement Xb and Xs respectively represent the strain in the BP and the SAS. Similar to CIBIC, the mass was set at 1.0 kg for simplicity and the model parameters were determined such that Xb and Xs predict the MPS in the BP and the SAS of the FE head/brain model. The model parameters determined included K_{b0}, K_{b1}, K_{s0}, K_{s1}, C_{b1} and C_{s1} (Figure 1).

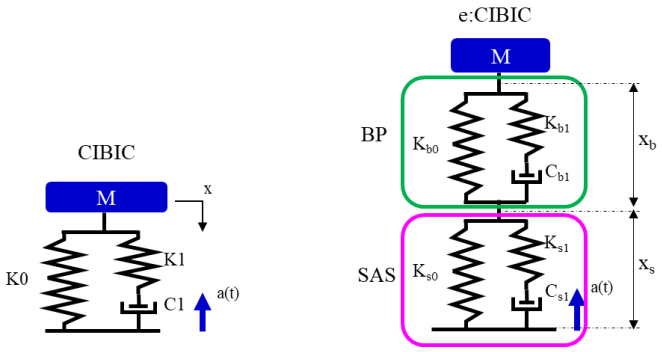

Figure 1. Comparison of the linear viscoelastic model used for CIBIC and e:CIBIC

Simplified rotational acceleration time histories were determined from actual impact test results to eliminate abnormal wave profiles. Ten full-frontal impact tests and ten moving deformable barrier side impact tests, each five of them coming from the largest and smallest peak head rotational acceleration groups, were chosen from the NHTSA vehicle crash test database [13]. In addition, ten car-pedestrian impact simulations were taken from those used in our previous study [5], each five of them coming from each of the largest and smallest peak head rotational acceleration groups. For all of these three impact configurations, the peak values were determined by the maximum of the three peak values in three rotational axes. The resulting thirty time histories were subjected to fast Fourier transform to determine distribution of the frequency and the amplitude. The frequency range was determined from the overall maximum and minimum value of the frequency range of each of the time histories determined between 90% and 100% of the maximum amplitude. The peak rotational acceleration was set at 5000 rad/s^2 by referring to the average value of the time histories used for the validation of the e:CIBIC in a later step. Three different simplified time histories were determined such that 1. the amplitude is the same for the entire frequency range, 2. the amplitude at the minimum frequency is ten times as much as the amplitude at the maximum frequency and 3. the amplitude at the maximum frequency is ten times as much as the amplitude at the minimum frequency (Figure 2). The resulting simplified rotational acceleration time histories are presented in Figure 3. These three simplified load cases are denoted as SLC 1 through 3.

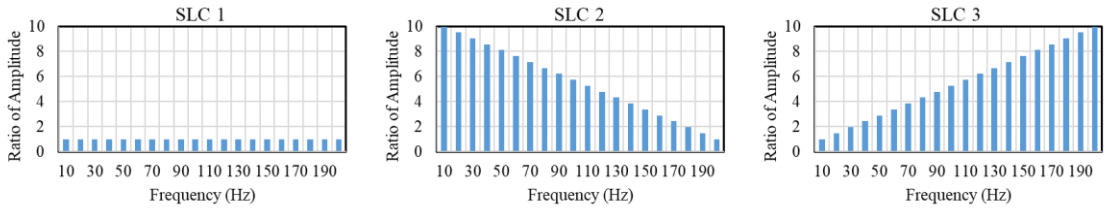

Figure 2. Distribution of amplitude by frequency

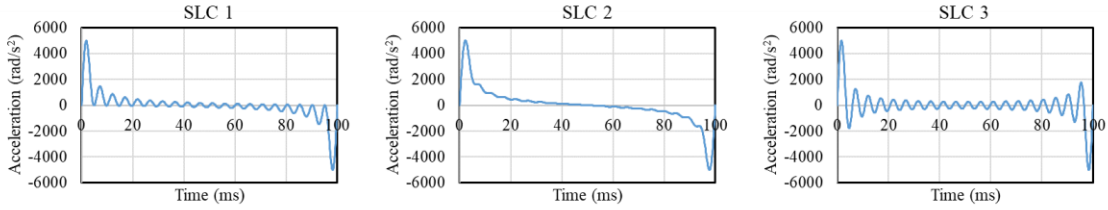

Figure 3. Simplified rotational acceleration time histories

These time histories were applied to both the e:CIBIC and the Global Human Body Models Consortium (GHBMC) head/brain model [9]. Rigid constraint was applied to the skull, mandible and flesh/skin of the GHBMC head/brain model with the prescribed acceleration time history applied to each of the three rotational axes (Figure 4). The rotational axes defined for this study are also illustrated in the figure. A numeric computing platform (MATLAB [14]) was controlled by an optimization software package (modeFRONTIER [15]) to optimize the model parameters of e:CIBIC using the optimization algorithm of MOGA-II. Due to the difference in the dimension of the MPS predicted by the FE head/brain model and X_b and X_s predicted by e:CIBIC, the time histories were normalized by their peak values and used for the optimization. Optimization was performed such that the summation of the CORA (CORrelation and Analysis) metric defined by the ISO/TS18571 [16] calculated for each of the six combinations of the three simplified rotational acceleration time histories and the two injury metrics (MPS in the BP and the SAS) is maximized for the normalized time histories. In addition to the determination of the model parameters, scaling factors S_b and S_s were determined to allow estimation of the MPS predicted by the FE head/brain model from the displacement calculated by the e:CIBIC criterion by dividing the peak value of the MPS from the FE head/brain model by the peak value of the displacement from the e:CIBIC criterion. The scaling factors were determined for each of the three simplified load cases and averaged to determine the final values to be used with the e:CIBIC criterion.

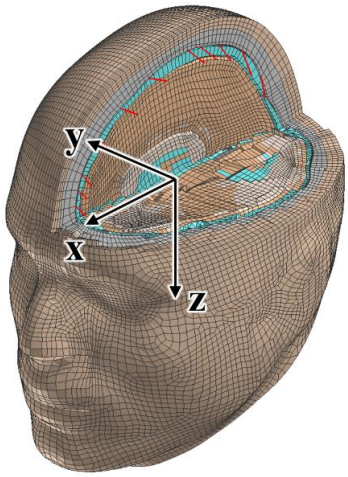

Figure 4. Schematic of the GHBMC head/brain model

Application of convolution integral

The convolution integral originally used to calculate the CIBIC criterion was applied to the calculation of the e:CIBIC criterion. The previous study to develop the CIBIC criterion [5] has found that in the current application, an impulse response can be well represented by the response to the step function with 1 ms duration. For this reason, the response of the e:CIBIC criterion to the step function with 1 ms duration was calculated for each of the three axes using MATLAB. Then the response in each of the three axes obtained was used to calculate e:CIBIC for a given rotational acceleration time history by means of the convolution integral. The e:CIBIC criterion is now defined using the following equations:

$$MPS_{BP} = S_b \sqrt{\sum_{i=1}^{3} \left\{ \int_0^t X_{bi}(t-\tau)\alpha_i(\tau)d\tau \right\}^2} \Bigg|_{max} \quad \text{Equation (1)}$$

$$MPS_{SAS} = S_s \sqrt{\sum_{i=1}^{3} \left\{ \int_0^t X_{si}(t-\tau)\alpha_i(\tau)d\tau \right\}^2} \Bigg|_{max} \quad \text{Equation (2)}$$

where MPS_{BP} and MPS_{SAS} denote the MPS in the BP and the SAS, respectively, S_b and S_s denote the scaling factor for the BP and the SAS, respectively, X_b and X_s denote the impulse response of the MPS in the BP and the SAS, respectively, α denotes the rotational acceleration, and $i = 1, 2, 3$ represent the x, y and z axis. The calculation was performed for the three simplified rotational acceleration time histories used to determine the model parameters to compare against the time history of e:CIBIC obtained by mean of MATLAB computation to make sure that the convolution integral used for the CIBIC criterion also works with the e:CIBIC criterion.

Validation

The model parameters determined for e:CIBIC were validated against the same GHBMC head/brain model in a number of different load cases in terms of both the correlation of peak values and the representation of time histories for the MPS in the BP and the SAS predicted by the GHBMC model.

The acceleration time histories of the head from the crash tests and simulations were prepared for the validation of the model parameters. ISO/TR19222 [17] assessed a number of different head injury metrics to predict the MPS in the brain subjected to rotational acceleration using the load cases from a variety of data sources. Of those, 71 full-frontal, 49 oblique frontal and 64 moving deformable barrier side impact tests that are currently available in the NHTSA database [13] were used. In addition, 62 pedestrian impact simulations performed by Takahashi et al. [5] were also referred to, resulting in 246 sets of head acceleration time histories in total. The crash tests and simulations used to determine the simplified head rotational acceleration time histories to determine model parameters were not included in the validation load cases.

Using the 246 load cases, the peak values of the MPS in the BP were plotted between the GHBMC head/brain model and the CIBIC criterion, and between the GHBMC head/brain model and the e:CIBIC criterion, respectively. Similarly, the peak values of the MPS in the SAS were plotted between the GHBMC head/brain model and the e:CIBIC criterion. The coefficient of determination (R^2) was calculated for each of the three plots to evaluate prediction capability of the e:CIBIC criterion relative to the 3D head/brain model and the CIBIC criterion. In addition, the CORA metric defined by ISO/TS18571 [16] was calculated for each of the 246 sets of the head rotational acceleration time histories between the GHBMC model and each of the CIBIC and the e:CIBIC criterion for the time history of the MPS in the BP, and between the GHBMC model and the e:CIBIC criterion for the time history of the MPS in the SAS. For each of the prediction models and the strain measure, the CORA scores obtained was averaged over all the load cases included in each of the four loading configurations (full-frontal, oblique-frontal, moving deformable barrier side and pedestrian impacts), as well as the grand total of 246 load cases and compared to each other to further validate the prediction capability of the e:CIBIC criterion.

RESULTS

Determination of model parameters

Figures 5 and 6 respectively compare the time histories of the MPS in the BP and the MPS in the SAS for the three rotational axes and the three simplified head acceleration time histories. The solid and the dotted curve represent the results from the e:CIBIC criterion and the GHBMC model, respectively. The six model parameters determined for the e:CIBIC criterion by averaging the optimized values over the three different simplified acceleration time histories are summarized in Table 1.

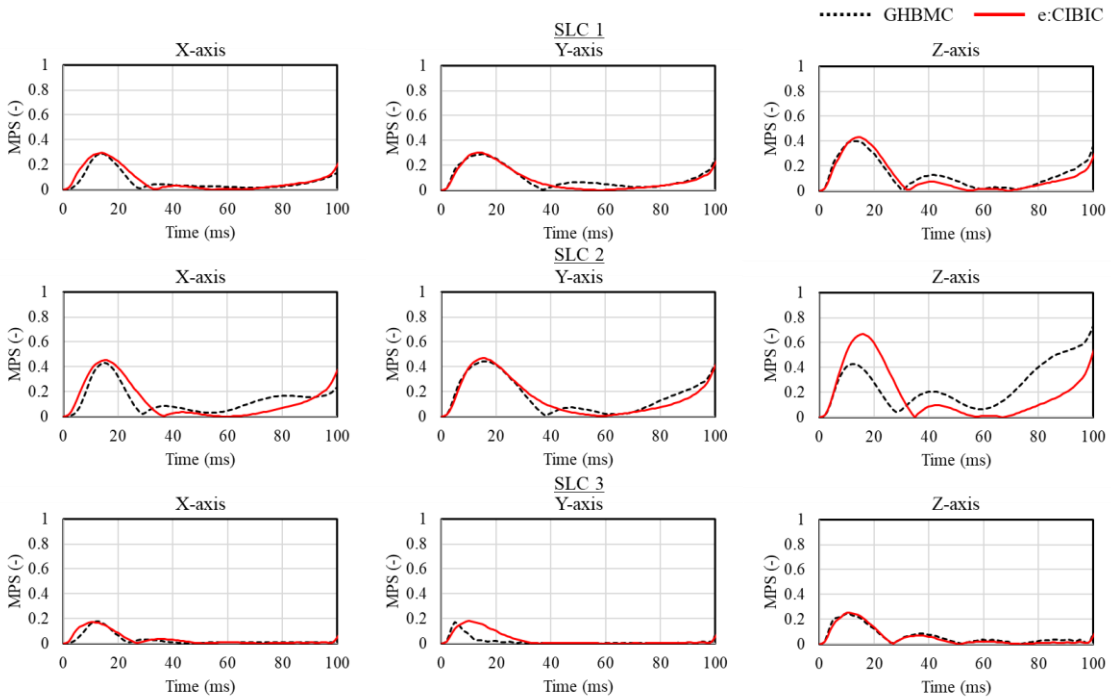

Figure 5. Comparison of the time history of the MPS in the BP between the GHBMC model and e:CIBIC

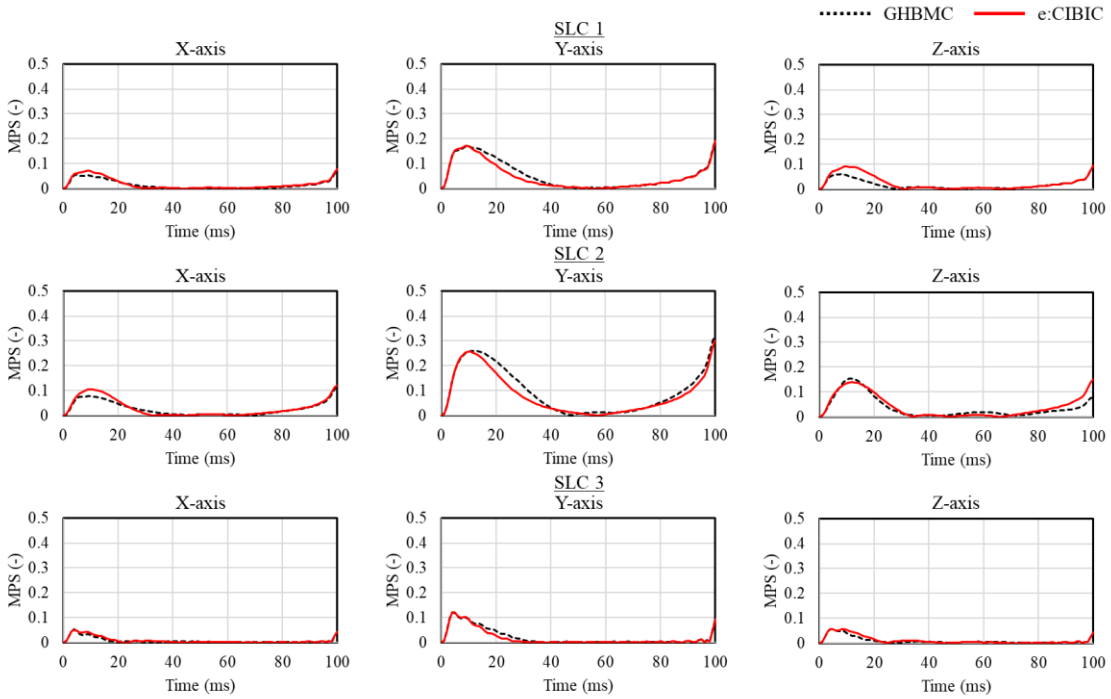

Figure 6. Comparison of the time history of the MPS in the SAS between the GHBMC model and e:CIBIC

Table 1.
Model parameters and scaling factors for e:CIBIC

Axis	K_{b0} (N/m)	K_{b1} (N/m)	C_{b1} (Ns/m)	K_{s0} (N/m)	K_{s1} (N/m)	C_{s1} (Ns/m)	Scaling Factor for BP	Scaling Factor for SAS
X	2.03E+04	1.46E+06	1.27E+02	2.82E+05	1.22E+05	1.83E+03	4.47	1.44E+01
Y	1.86E+04	4.99E+05	1.96E+02	1.31E+05	1.82E+05	9.98E+02	5.49	1.94E+01
Z	1.97E+04	6.36E+05	1.08E+02	1.69E+05	1.14E+05	1.24E+03	6.06	1.44E+01

Application of convolution integral

Figure 7 shows the time histories of the impulse response for both the MPS in the BP and the MPS in the SAS for x, y and z axis represented by the response to the 1 ms duration step function of the rotational acceleration time histories with the magnitude of 1.0 rad/s^2. Figure 8 presents the comparison of the time histories of the MPS in the BP and the SAS between the e:CIBIC criterion calculated using the convolution integral and the e:CIBIC calculated using MATLAB for the three simplified head acceleration time histories. The solid and dotted curves respectively represent the convolution integral and MATLAB calculation. The time histories are plotted for the resultant of the three axes.

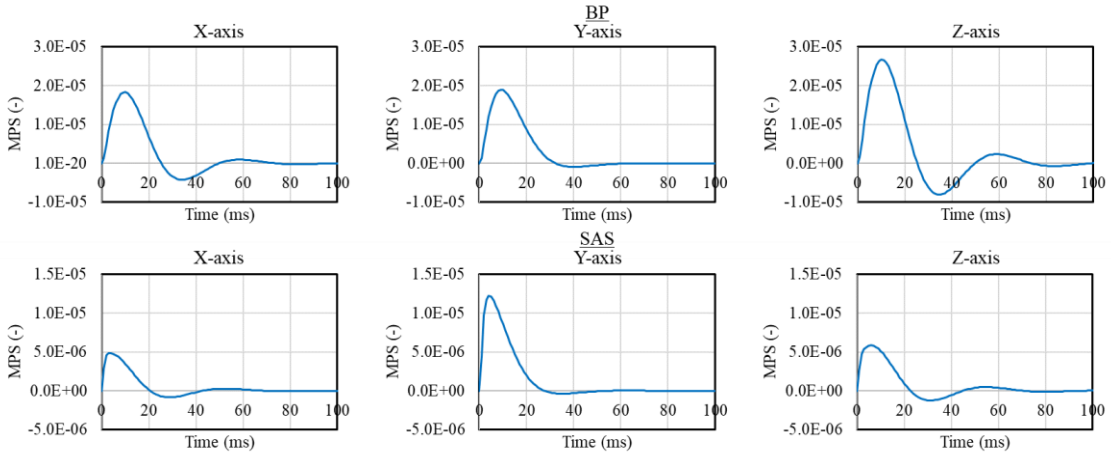

Figure 7. Impulse response of the MPS in the BP and the MPS in the SAS

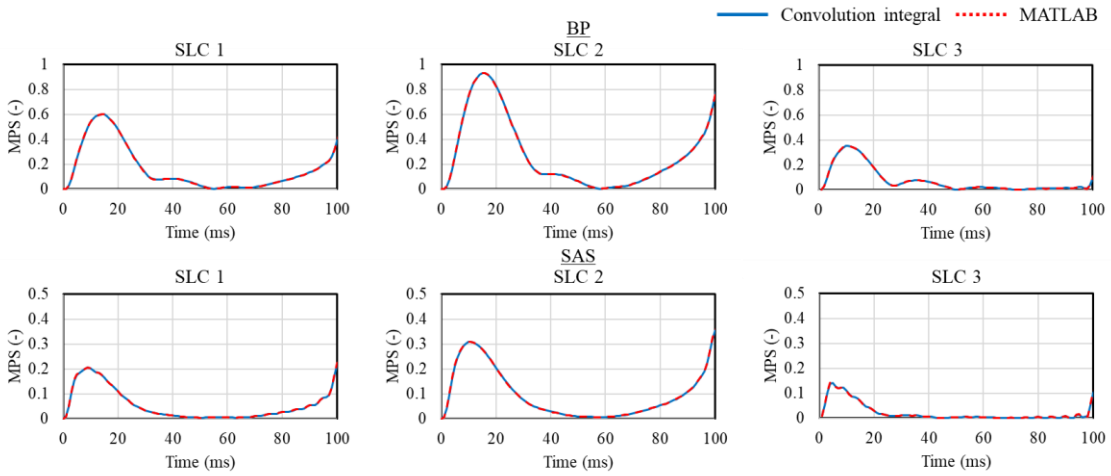

Figure 8. Comparison of the time history of the MPS in the BP and the SAS calculated using convolution integral and MATLAB

Validation

Figure 9 plots the correlation of the peak resultant values of the MPS for the load cases used for the validation. As for the MPS in the BP, the results obtained from the GHBMC model is plotted against both the CIBIC criterion and the e:CIBIC criterion, while the GHBMC model results are plotted only against the e:CIBIC for the MPS in the SAS due to the lack of prediction of the MPS in the SAS with the CIBIC criterion. Comparisons were made for all of the 246 load cases used, along with each one of the four impact configurations (full-frontal, oblique-frontal, moving deformable barrier side and pedestrian impact). Table 2 summarizes the coefficient of determination (R^2) obtained from each of the correlation plots presented in Figure 9.

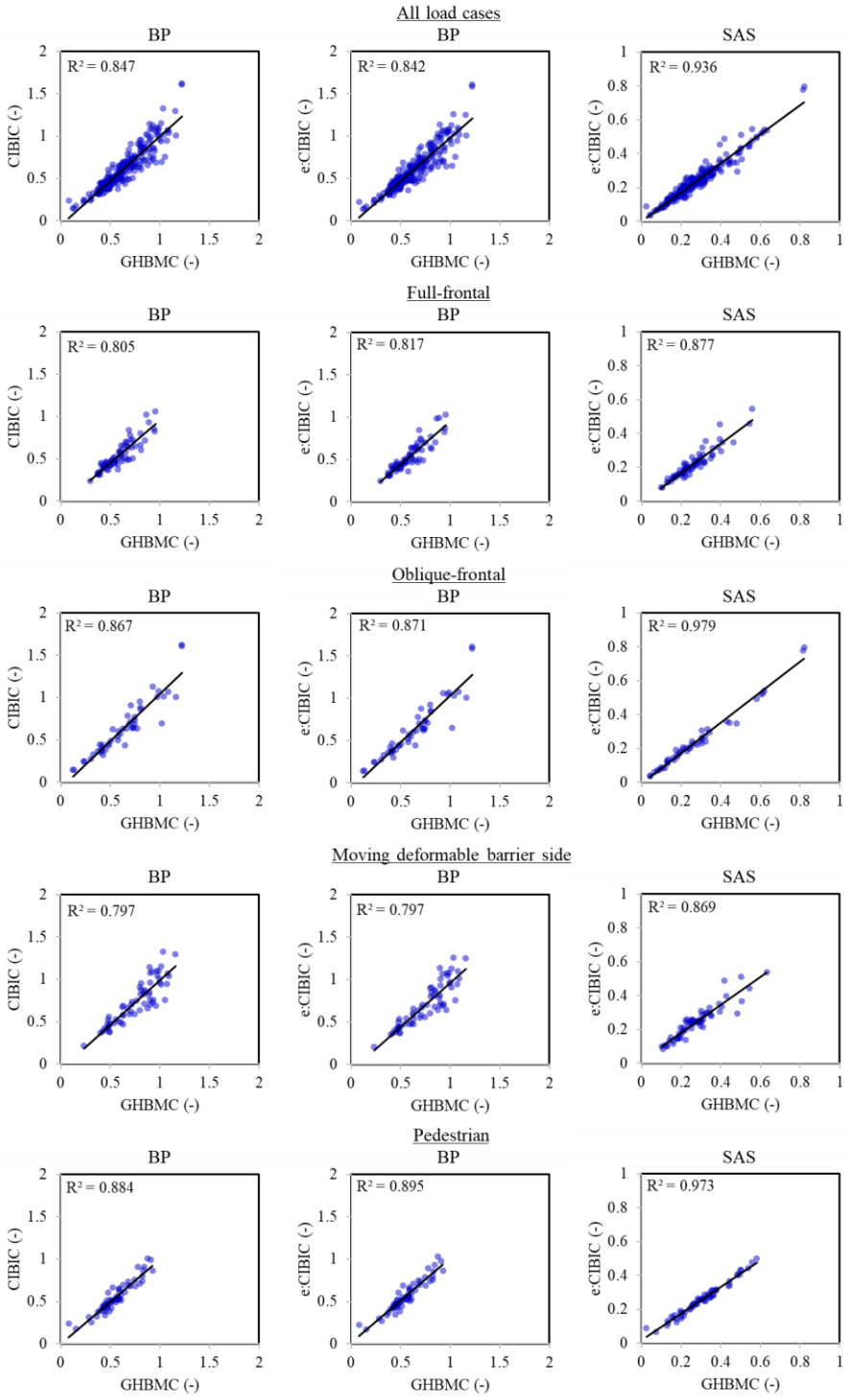

Figure 9. Correlation plots of the peak resultant value of the MPS between the GHBMC model and CIBIC/e:CIBIC

Table 2.
Summary of coefficient of determination (R^2)

Load case	MPS in BP GHBMC v.s. CIBIC	MPS in BP GHBMC v.s. e:CIBIC	MPS in SAS GHBMC v.s. e:CIBIC
All load case	0.847	0.842	0.936
Full-Frontal	0.805	0.817	0.877
Oblique-frontal	0.867	0.871	0.979
MDB side	0.797	0.797	0.869
Pedestrian	0.884	0.895	0.973

Figures 10 through 12 respectively compare the time histories of the MPS in the BP predicted by the CIBIC criterion, the MPS in the BP predicted by the e:CIBIC criterion and the MPS in the SAS predicted by the e:CIBIC criterion, all against those predicted for the corresponding measure by the GHBMC head/brain model. The solid and the dotted curve represent the results from the injury criteria and those from the GHBMC head/brain model, respectively. Comparisons were made for one exemplar load case chosen from each of the full-frontal, oblique-frontal, moving deformable barrier side and pedestrian impact load cases used for validation. For each of these three comparisons, Table 3 summarizes the average of the CORA metric over all the load cases included in each of the four crash configurations along with the overall average of the 246 load cases.

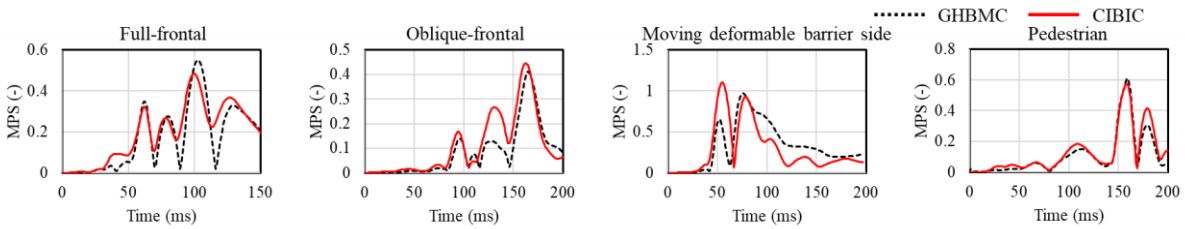

Figure 10. Comparison of the time history of the MPS in the BP between CIBIC and the GHBMC model

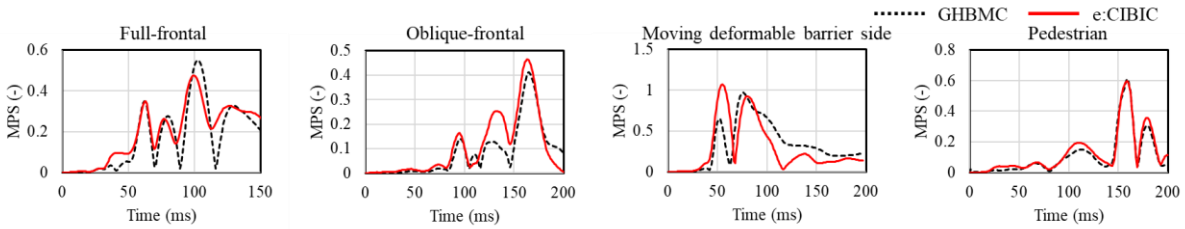

Figure 11. Comparison of the time history of the MPS in the BP between e:CIBIC and the GHBMC model

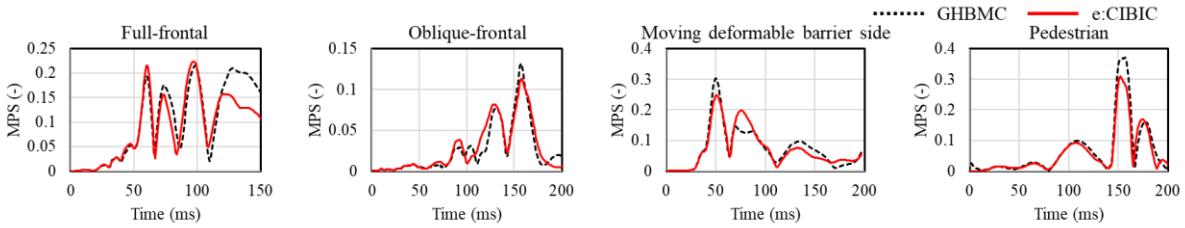

Figure 12. Comparison of the time history of the MPS in the SAS between e:CIBIC and the GHBMC model

Table 3.
Summary of the average value of the CORA metric

Load case	MPS in BP GHBMC v.s. CIBIC	MPS in BP GHBMC v.s. e:CIBIC	MPS in SAS GHBMC v.s. e:CIBIC
All load case	0.736	0.733	0.852
Full-Frontal	0.741	0.735	0.861
Oblique-frontal	0.728	0.728	0.833
MDB side	0.657	0.658	0.840
Pedestrian	0.819	0.815	0.872

DISCUSSION

In an effort to predict rupture of the BV and subsequent ASDH, a methodology of prediction using a practical, kinematics-based injury criterion was investigated. To the best of the authors' knowledge, this is the first attempt to establish such a simplified injury criterion to predict strains in the BP and the SAS simultaneously. As the first step, the existing CIBIC criterion was extended to incorporate one more SLS in series to predict the MPS in the SAS, in addition to the MPS in the BP, given the assumption that the strain in the SAS is significantly related to the strain in the BVs due to strong connection between the SAT and the blood vessels running through the SAS. The results of the current study showed that this extended version of the CIBIC criterion, e:CIBIC, succeeded in simultaneously predicting both the MPS in the BP and the MPS in the SAS predicted by the GHBMC with a simplified model, while maintaining the prediction capability of the CIBIC criterion for the MPS in the BP, as summarized in Tables 2 and 3 for the coefficient of determination of the peak MPS correlation and the average CORA metric of the MPS time histories, respectively. Although promising results have been obtained in comparison with a specific full-FE head/brain model, it should be noted that the validity of the results largely depends on the validity of such head/brain model against which the model parameters are optimized. Further improvement of the kinematics-based simplified injury criterion needs to be considered as the full-FE head/brain models are improved.

The current study validated the e:CIBIC criterion with the model parameters optimized in three simplified load cases against a total of 246 head impacts from pedestrian, oblique-frontal, full-frontal and moving deformable barrier side crash tests or simulations. The results of the validation generally showed a trend of degradation of the prediction capability in this order of the impact configurations. This can be endorsed by the exemplar acceleration time histories presented in Figure 13. For each of the rotational acceleration time history plot, the rotational axis most relevant to the corresponding impact configuration was chosen (X-axis for pedestrian and MDB side, Y-axis for oblique-frontal and full-frontal). The duration superimposed on each of the plot represents the wavelength of the single or combined peak of the rotational acceleration deemed responsible for the largest peak response. The wavelengths were found to be approximately 15, 22, 65 and 70 ms for pedestrian, oblique-frontal, full-frontal and MDB side impact configurations, indicating that the prediction capability is degraded as the wavelength of the relevant peak goes up. Despite that the e:CIBIC criterion is based on the SLS that represents a viscoelastic material response, one set of the SLS only includes one single damping coefficient, which means that only one time constant is represented by each of the SLS. This would reduce the prediction capability as the impact duration becomes longer and a wider range of the frequency components is involved. A future study may need to consider the increase in the number of time constants represented in the simplified viscoelastic model.

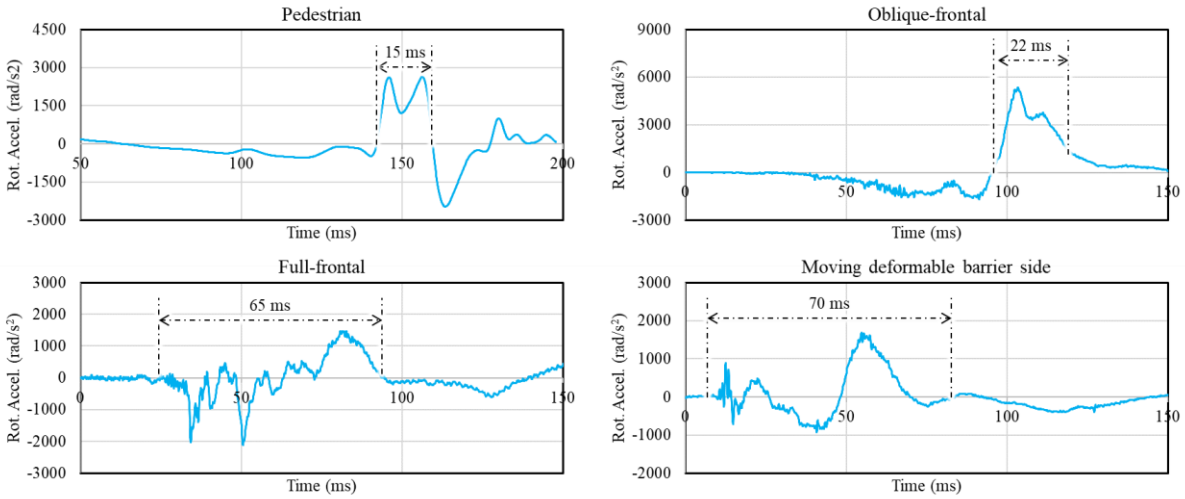

Figure 13. Rotational acceleration time histories of the head about the most relevant axis

The next step towards the ultimate goal of predicting the damage to the BP and the acute subdural hematoma with a practical simplified injury criterion, a detailed FE model of the head/brain that incorporate accurate geometry, material property and boundary conditions needs to be used to clarify and quantify the influence of the strain in the SAS on the strain in the BV. Once such clarifications are given and the relationship between the strain in the SAS and the strain in the BV is established, the combination of the assessment criteria of both the head linear acceleration (such as HIC) and the rotational acceleration (such as e:CIBIC) would allow prediction of a variety of different brain injury types, including contusion, epidural hemorrhage, concussion/diffuse axonal injury, brain swelling and acute subdural hematoma.

CONCLUSIONS

In this study, the rotational brain injury criteria to predict the MPS in the BP, the CIBIC criterion, was enhanced by implementing another set of the SLS model in series to predict the MPS in the SAS in addition to the MPS in the BP. As a result, the following conclusions were reached:

- The six model parameters of the e:CIBIC criterion optimized for the three simplified head rotational acceleration time histories resulted in the coefficient of determination of 0.846 and 0.936 against the GHBMC head/brain model for the peak values of the MPS in the BP and the MPS in the SAS, respectively, in the validation using a total of 246 crash tests and simulations that included four different impact configurations.
- The results compared against the CIBIC criterion with the coefficient of determination of 0.849 for the MPS in the BP, showing that the e:CIBIC criterion is capable of predicting the MPS in the SAS, while maintaining the predictive capability of the CIBIC criterion for the MPS in the BP.
- The overall average CORA metric obtained from the model validation were 0.732 and 0.852 against the GHBMC head/brain model for the time histories of the MPS in the BP and the MPS in the SAS, respectively, confirming the same trend as that of the peak MPS correlation against the CIBIC criterion that yielded the overall average CORA metric of 0.734 for the MPS in the BP.
- The validation results for each of the impact configurations showed a generic trend of degradation in the predictive capability as the wavelength of the rotational acceleration time history responsible for the overall peak response becomes longer, requiring further investigations on the influence of the number of time constants represented by the model.

REFERENCES

[1] International Transport Forum. 2021. “Road Safety Annual Report 2021: The Impact of Covid-19.” OECD Publishing, Paris.

[2] National Police Agency. (2022, March 3). Table Number 1-3, Trends in traffic accidents by year (1948-2021). Traffic Accident Statistics, Annual Report 2021 (Traffic accidents). https://www.npa.go.jp/publications/statistics/koutsuu/toukeihyo_e.html

[3] National Police Agency. (2022, March 3). Table Number 2-4-2, Casualties by major part of physical damage and road user type. Traffic Accident Statistics, Annual Report 2021 (Serious accidents). https://www.npa.go.jp/publications/statistics/koutsuu/toukeihyo_e.html

[4] Li, M., Zhao, Z., Yu, G. and Zhang, J. 2016. “Epidemiology of traumatic brain injury over the world: a systematic review.” General medicine: open access 2016; 4(5): e275

[5] Takahashi, Y. and Yanaoka, T. 2017. “A study of injury criteria for brain injuries in traffic accidents.” In proceedings of the 25th ESV conference (Detroit, MI, USA, June 5-8), paper number 17-0040

[6] Holbourn, A.H.S. 1943. “Mechanics of head injuries.” Lancet 2. October 9: 438–41

[7] Laic, R., Kapeliotis, M., Famaey, N., Depreitere, B., Kleiven, S. and Sloten, J. 2021. “Quantifying biovariability in position and diameter of bridging veins to improve acute subdural hematoma prediction in FE head models.” In proceedings of the IRCOBI conference 2021 (online), paper number IRC-21-41

[8] Fernandes, S., Sousa, R. and Ptak, M. 2021. “Numerical Aspects of Subdural Haematoma Modeling and Prediction.” In proceedings of the IRCOBI conference 2021 (online), paper number IRC-21-43

[9] Mao, H., Zhang, L., Jiang, B., Genthikatti, V.V., Jin, X., Zhu, F., Makwana, R., Gill, A., Jandir, G., Singh, A., Yang, K.H. 2013. “Development of a finite element human head model partially validated with thirty five experimental cases.” J Biomech Eng., 135(11): 111002

[10] Gabler, L., Crandall, J. and Panzer, M.. 2019. “Development of a Second-Order System for Rapid Estimation of Maximum Brain Strain.” Ann Biomed Eng. 2019 Sep; 47(9):1971-1981

[11] Shafique, S., Rayi, A. 2022. “Anatomy, Head and Neck, Subarachnoid Space. [Updated 2022 Aug 8].” In: StatPearls [Internet] (StatPearls Publishing, Treasure Island, FL, 2022 Jan-). https://www.ncbi.nlm.nih.gov/books/NBK557521/

[12] Mortazavi, M., Quadri, S., Khan, M., Gustin, A., Suriya, S., Hassanzadeh, T., Fahimdanesh, K., Adl, F., Fard, S., Taqi, M., Armstrong, I., Martin, B. and Tubbs, R. 2018. “Subarachnoid Trabecurae: A Comprehensive Review of Their Embryology, Histology, Morphology, and Surgical Significance.” World Neurosurg. (2018) 111:279-290

[13] National Highway Traffic Safety Administration. “Vehicle Crash Test Database.” https://www.nhtsa.gov/research-data/research-testing-databases#/vehicle

[14] MathWorks. 2019. “MATLAB/Simulink.” https://jp.mathworks.com/products/simulink.html

[15] ESTECO SpA. 2022. “modeFRONTIER.” https://engineering.esteco.com/modefrontier/

[16] ISO. 2014. “ISO/TS 18571:2014 Road vehicles - Objective rating metric for non-ambiguous signals”

[17] ISO. 2021. “ISO/TR 19222:2021 Road vehicles - Injury risk curves for the THOR dummy”